nature communications

Article

https://doi.org/10.1038/s41467-024-54571-w

Lenalidomide-induced pure red cell aplasia is associated with elevated expression of MHC-I molecules on erythrocytes

Received: 26 February 2024

Accepted: 15 November 2024

Published online: 22 November 2024

Check for updates

Qi Hu[1,2,7], Yang Liu[3,7], Qiuyu Yue[1,2], Shuo Zhou[1,2], Xianghong Jin[4], Fan Lin[3], Xiao-Jun Huang[2,3], Junling Zhuang[4] ✉, Jin Lu[3] ✉, Xiaofei Gao[5,6] ✉ & Hsiang-Ying Lee[1,2,3] ✉

The RVd therapy, combining lenalidomide, bortezomib, and dexamethasone, is a mainstay treatment for multiple myeloma. A multiple myeloma patient developed pure red cell aplasia (PRCA) following RVd treatment, despite the absence of common PRCA triggers. In vitro analyses reveal lenalidomide as a pivotal disruptor of erythropoiesis. Single-cell transcriptome analysis unveils hyperactive $CD8^+$ T cells and impaired erythropoiesis in the patient's bone marrow. Unexpectedly, the patient's erythroid cells display abnormally high expression of genes in the antigen presentation pathway, particularly those for major histocompatibility class I (MHC-I) molecules. Functional assays demonstrate that lenalidomide treatment further augmented MHC-I expression in the patient's erythroid cells. Blocking MHC-I or depleting T cells alleviates the defective erythropoiesis of PRCA, suggesting that the interaction between erythroid cells with elevated MHC-I and T cells in the bone marrow might contribute to PRCA. Taken together, our study implicates a mechanism underlying lenalidomide-induced PRCA in treating cancer patients.

Pure red blood cell aplasia (PRCA) is a rare hematological disorder characterized by near absence of erythroblasts in the bone marrow and impairment of erythropoiesis[1,2]. Acquired PRCA may be associated with various factors, including immune disorders, B19 parvovirus infection[3,4], antibodies triggered by recombinant human erythropoietin, thymoma, and lymphoproliferative disorders (e.g., chronic lymphocytic leukemia and large granular lymphocyte leukemia)[2,5–8]. Furthermore, over 50 drugs and chemicals have been associated with the onset of PRCA[9–11]. Nonetheless, the mechanisms underlying most drug-induced PRCA remain elusive.

RVd therapy, comprising lenalidomide, the proteasome inhibitor bortezomib, and the glucocorticoid dexamethasone, has been approved as the preferred treatment regimen for the majority of multiple myeloma (MM) patients[12–15]. Anemia frequently afflicts individuals with MM[16]. Previous clinical reports have consistently shown significant reductions in M protein levels and the number of myeloma cells following RVd treatment[13,17,18], often coinciding with the remission of anemia. Apart from that, lenalidomide, an immunomodulatory drug, has also been widely used in the treatment of patients with 5q-myelodysplastic syndrome[19]. It modulates the host immune system to promote the immune-mediated clearance of

[1]Ministry of Education Key Laboratory of Cell Proliferation and Differentiation, School of Life Sciences, Peking University, Beijing 100871, China. [2]Peking-Tsinghua Center for Life Sciences, Academy for Advanced Interdisciplinary Studies, Peking University, Beijing 100871, China. [3]Peking University People's Hospital, Peking University Institute of Hematology, National Clinical Research Center for Hematologic Disease, Beijing 100871, China. [4]Department of Hematology, Peking Union Medical College Hospital, Chinese Academy of Medical Sciences, Beijing, China. [5]Key Laboratory of Growth Regulation and Translational Research of Zhejiang Province, School of Life Sciences, Westlake University, Hangzhou 310030 Zhejiang, China. [6]Westlake Laboratory of Life Sciences and Biomedicine, Hangzhou, Zhejiang, China. [7]These authors contributed equally: Qi Hu, Yang Liu. ✉e-mail: zhuangjunling@pumch.cn; jin1lu@sina.com; gaoxiaofei@westlake.edu.cn; slee@pku.edu.cn

cancer cells by inducing T-cell costimulation and proliferation, as well as increasing the production of interleukin (IL)-2 and interferon (IFN) γ[20–22] Additionally, lenalidomide was identified to bind to the CRBN-CRL4 E3 ubiquitin ligase. It functions in multiple myeloma by promoting the ubiquitination of two transcription factors, IKZF1 and IKZF3, and the degradation of casein kinase 1A1 (CK1α), leading to clinical efficacy in del(5q) MDS[23,24].

A few clinical cases have documented recurrent PRCA induced by lenalidomide in patients with myelodysplastic syndrome[25] or multiple myeloma[26]; however, the mechanisms underlying lenalidomide-induced PRCA have not been elucidated. Here, we present a case of a multiple myeloma patient who, after undergoing three courses of RVd treatment, developed PRCA. This condition was characterized by a paucity of erythroid progenitors in the bone marrow, a hemoglobin level of 50 g/L, and a reticulocyte percentage of 0.04%. Clinical assessment of this patient ruled out the common underlying conditions leading to PRCA, therefore indicating the association between the RVd treatment and the development of PRCA.

In this study, we comprehensively employed single-cell transcriptome analysis, proteomic analysis and functional assays to continuously monitor the cellular status of the case under investigation. The functional assays revealed a key role of lenalidomide, as opposed to bortezomib or dexamethasone, in the development of PRCA in this patient. We not only identified hyperactive $CD8^+$ T cells, which likely inflicted the injury on erythroid progenitors, but also found that the patient's erythroblasts showed elevated MHC-I expression, a phenomenon induced by lenalidomide. The drug-induced augmentation of MHC-I on erythroblasts is associated with the development of PRCA and may serve as a biomarker for other clinical PRCA conditions. Overall, our findings illuminate the potential mechanism underlying drug-induced PRCA and provide insights concerning the roles of aberrant erythroid progenitors in affected individuals.

Results

Clinical manifestations of drug-induced PRCA in a patient with multiple myeloma

This study presents the case of a rare patient with multiple myeloma (Table 1). Anemia was noted during routine examination, with a hemoglobin level of 82 g/L and a reticulocyte count of 0.0351×10^9/mL (reference range: $0.024–0.084 \times 10^9$/mL). At this juncture, the bone marrow exhibited active erythroid hyperplasia, characterized by a granular/erythroid cell ratio of 3.4:1. The patient underwent three cycles of RVd therapy and achieved a very good partial response (VGPR). Pathological examination of a bone marrow aspirate specimen revealed the plasma cells dropped from 32.5% to 3.5%. However, the anemia persisted and worsened. Subsequent blood tests showed a drop in the hemoglobin level to 55 g/L, with a reticulocyte count of 0.0005×10^9/mL, and EPO levels exceeding 758 mIU/mL. The Coombs test was negative, and no paroxysmal nocturnal hemoglobinuria (PNH) clone was detected. Further bone marrow examination confirmed the absence of erythroid lineage cells, leading to the diagnosis of PRCA. We found no evidence of parvovirus, CMV, or EBV infection. Both bone marrow B cell and TCR-Vβ flow cytometry returned negative results. CT scans reveal no thymoma.

Initially, this patient responded well to immunosuppressant. After five months of treatment with cyclosporine A (CsA), the level of Hb was restored to 109 g/L, achieving partial remission. However, three months after suspension, the level of Hb dropped again to 40 g/L, with reticulocyte count of 0.0039×10^9/mL, and a ratio of 0.34%, all while erythroid lineage cells remained absent in the bone marrow. Consequently, allogeneic hematopoietic stem cell transplantation (allo-HSCT) was scheduled for administration.

Impaired erythropoiesis in PRCA patients is associated with lenalidomide treatment

To investigate the mechanism underpinning the onset of PRCA, we collected bone marrow samples from the patient during partial remission after CsA treatment (P3), at recurrence (P4), and during treatment failure (P5) (Fig. 1A). Notably, in contrast to the MM stage, bone marrow smears during the PRCA stage exhibited a virtual absence of erythroid precursors, consistent with the patient's clinical presentation (Fig. 1B). We observed a dramatic reduction in the percentage of $CD71^+CD235a^+$ erythroid precursors in the PRCA patient's bone marrow compared to that of healthy donors (HDs) (Fig. 1C, D). However, there were no significant differences in the percentages of KIT^+ hematopoietic stem and progenitor cells (HSPCs) (Fig. 1E; Supplemental Fig. 1A). Therefore, the impaired erythropoiesis was not attributable to a shortage of HSPCs. Although bone marrow mononuclear cells (BMMCs) from the PRCA patient could undergo erythroid differentiation, they developed substantially slower than cells from HDs, and the enucleation rate was also reduced (Fig. 1F, G; Supplemental Fig. 1B). Furthermore, the patient's erythroblasts displayed a severe decrease in their proliferative capacity (Fig. 1H). Colony-forming assays of the PRCA patient's BMMCs showed a substantial reduction in both the number and size of burst-forming units-erythroid (BFU-E) colonies, whereas the numbers of other myeloid colonies (CFU-GEMM, CFU-GM) were unaffected (Fig. 1I–K; Supplemental Fig. 1C). Collectively, our results indicated that the deficiency in erythropoiesis was attributable to a diminished number and impaired differentiation capacity of erythroid cells.

This patient had not been diagnosed with any common triggers of PRCA[1]. However, PRCA manifested after three courses of RVd treatment, implying a potential contribution of RVd drugs to its development. With the addition of RVd in the erythroid culture medium, both cells from HD and the PRCA patient exhibited a delay in erythroid differentiation compared to the control (DMSO treated). However, HD cells eventually underwent erythroid differentiation, achieving a significantly higher number of erythroid cells compared to the control. In contrast, PRCA cells showed severely impaired cell proliferation and differentiation (Supplemental Fig. 2A–C). To identify the specific drug responsible for PRCA, we systematically tested each component of the RVd regimen in a primary human erythroid culture (Fig. 2A–C; Supplemental Fig. 2D). Dexamethasone considerably increased erythroid proliferative capacity, consistent with previous reports[27]. Bortezomib had no discernible effect

Table 1 | Patient characteristics during disease progression

	Stage P1 Multiple myeloma	Stage P2 Initial onset of PRCA	Stage P3 Partial remission	Stage P4 PRCA recurrence	Stage P5 Cyclosporine treatment failure
M protein	18.1 g/L	0.4 g/L	0	0	1.6 g/L
Bone marrow plasma cells	32.50%	3.50%	3.00%	2.50%	2%
Bone marrow myeloid/erythroid ratio	3.4:1	124:0	16.22: 1	53.67:1	12:01
Hemoglobin level	82 g/L	55 g/L	69 g/L	42 g/L	56 g/L
Reticulocyte ratio	1.64%	0.03%	0.48%	0.32%	0.54%
Peripheral blood $CD8^+$ T cell count	–	801/μL	-	487/μL	467/μL
Peripheral blood $CD4^+$ T cell count	–	639/μL	-	378/μL	361/μL

https://doi.org/10.1038/s41467-024-54571-w

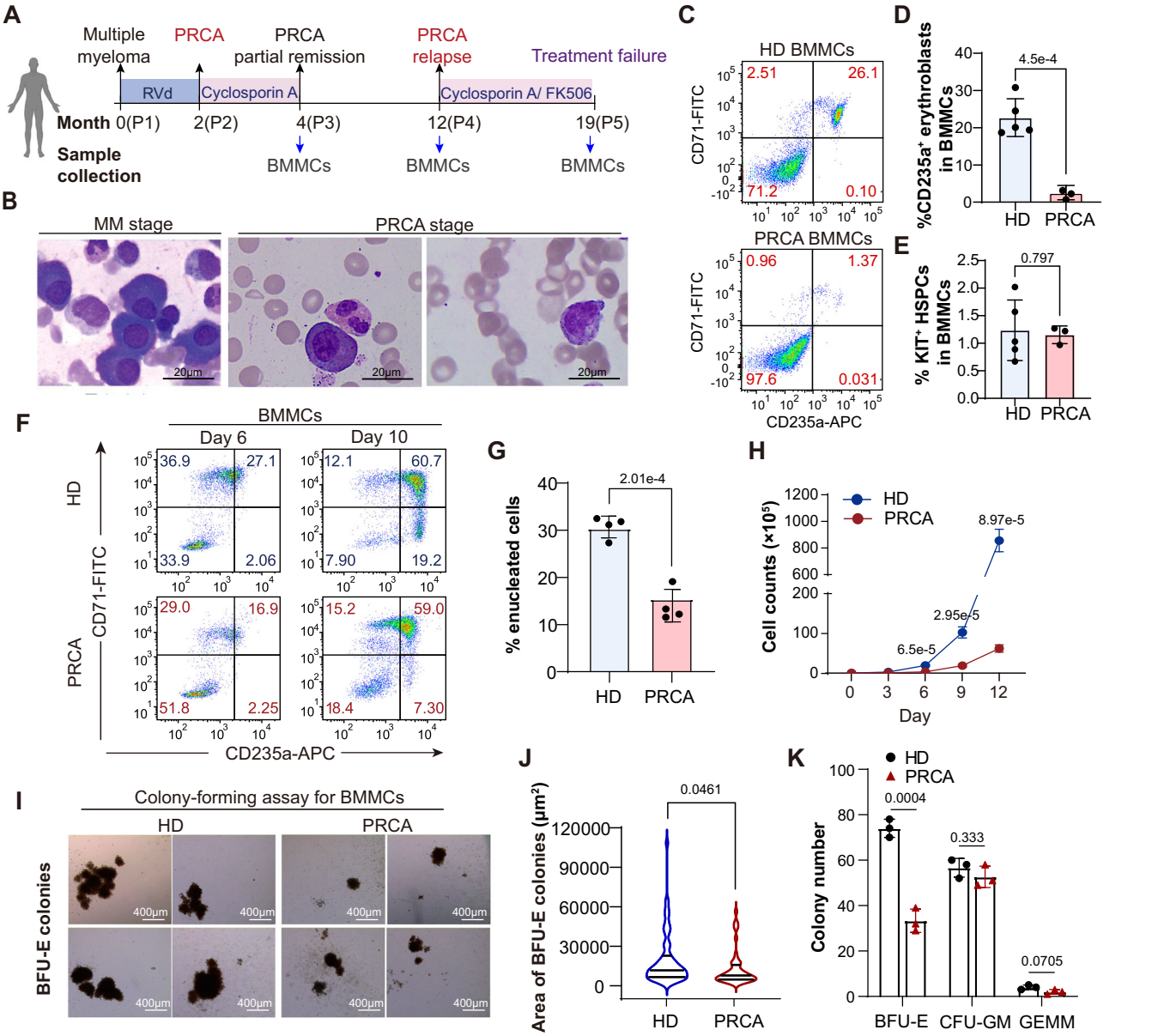

Fig. 1 | Clinical assessment and in vitro analysis of erythroid development in the PRCA patient. A Disease course and therapeutic regimen. **B** Morphology of cells in the patient's bone marrow at the MM stage (left) and the PRCA stage (right). Similar results were obtained based on 30 fields of view under the microscope for the patient's bone marrow smears at each stage. **C** Representative flow cytometry results showing percentages of erythroblasts in the bone marrow of healthy donors (HD, upper) and PRCA patients (lower). **D**, **E** Graphs quantifying percentages of erythroid precursors (**D**) and HSPCs (**E**) in HD ($n = 5$; samples from five individuals as biological replicates) and PRCA ($n = 3$; samples from three PRCA timepoints of the patient as biological replicates). Data are presented as mean values ± SEM. Two-tailed paired Student's t-test. **F** Flow cytometry analysis of BMMCs from the PRCA patient and HD undergoing ex vivo erythroid culture. Erythroid differentiation markers CD71 and CD235a were assessed on days 6 and 10. **G** Erythroid cell enucleation was analyzed by flow cytometry on day 14 ($n = 4$; biological replicates). Data are presented as mean values ± SEM. Two-tailed paired Student's t-test. **H** BMMCs from PRCA and HD were cultured in a serum-free erythroid medium. Cell numbers were counted every 3 days from three independent biological replicates. Data are presented as mean values ± SEM. Two-tailed paired Student's t-test. **I**–**K** Colony-forming assays were performed using BMMCs from HD (left) or PRCA (right). Representative micrographs of BFU-E colonies are shown in panel (**I**). Area of BFU-E colonies (**J**) and colony numbers of BFU-E, CFU-GM, and colony-forming unit-granulocyte, erythroid, macrophage, and megakaryocyte (CFU-GEMM) (**K**) were quantified ($n = 3$; biological replicates). Data are presented as mean values ± SEM. Two-tailed paired Student's t-test. Source data are provided as a Source Data file.

on the patient's BMMCs. Notably, lenalidomide exhibited a modest promotion of proliferation in cells from healthy donors but led to a substantial delay in erythroid differentiation and impairment of proliferation in the patient's cells. Moreover, lenalidomide induced a significant increase in apoptosis in the patient's cells (Fig. 2D, E). Consistently, the addition of lenalidomide profoundly reduced the number of BFU-E colonies but did not impact CFU-GM colonies (Fig. 2F, G; Supplemental Fig. 3A, B). Collectively, these findings strongly suggest that lenalidomide played a crucial role in inducing PRCA in this patient by specifically targeting erythropoiesis.

scRNA-Seq analysis revealed significant alterations in the percentages of multiple cell lineages in the bone marrow of PRCA

We next performed single-cell RNA-Seq (scRNA-Seq) analysis on BMMCs from HDs and the PRCA patient at stages of partial remission and recurrence (Fig. 3A, B). Analysis of cell composition revealed that the

https://doi.org/10.1038/s41467-024-54571-w

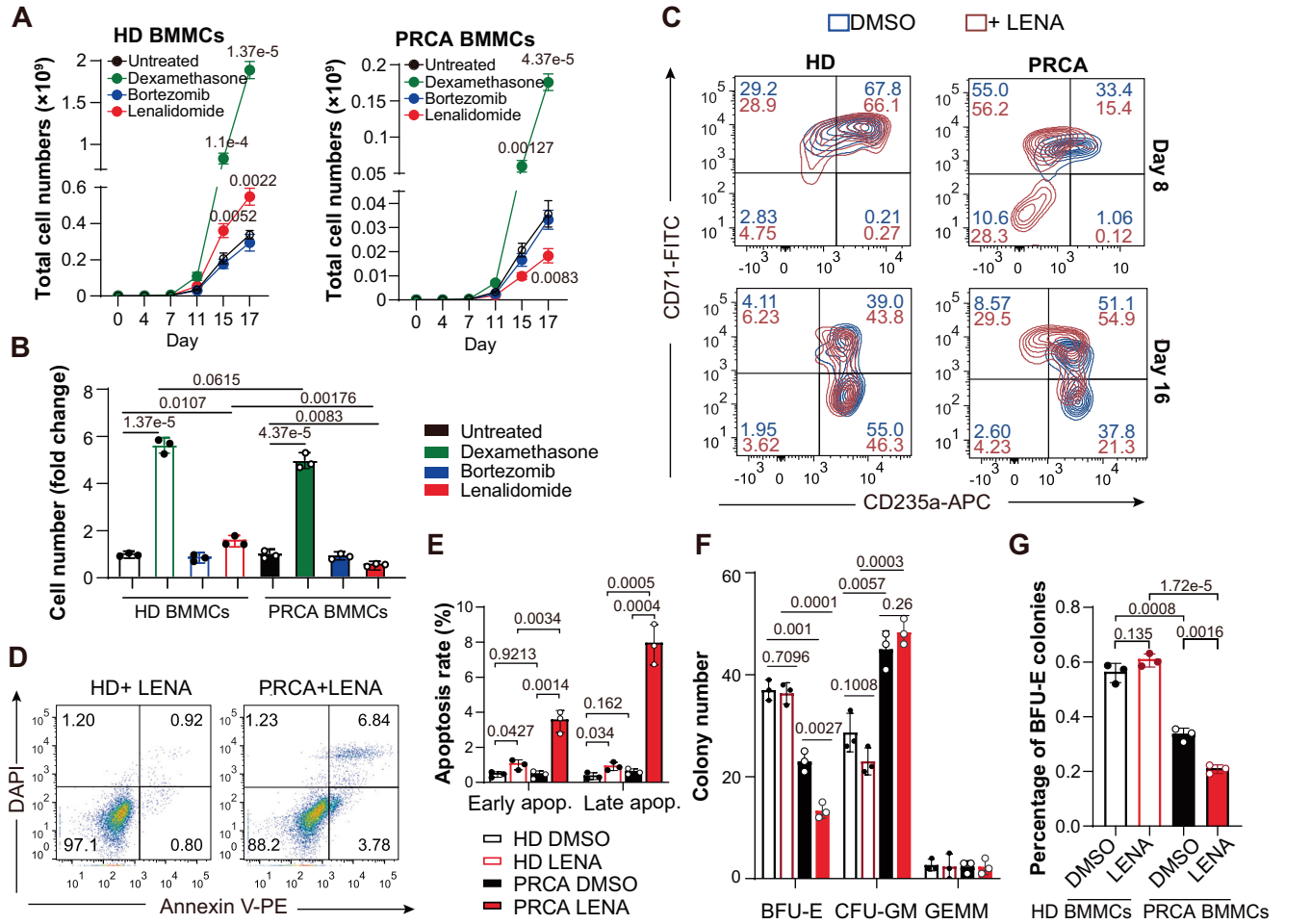

Fig. 2 | Lenalidomide has an inhibitory effect on in vitro erythroid development in cells from the PRCA patient. A BMMCs from healthy donors (HD, left) and PRCA (right) were cultured in a serum-free erythroid medium with indicated treatments. Cell numbers were counted every 4 days from three independent biological replicates. DMSO was added as the untreated control group. Data are presented as mean values ± SEM. Two-tailed paired Student's *t*-test. **B** Quantification of the impact of drugs on erythroid proliferation. The fold change indicates the drug's impact on the final number of erythrocytes from the same donor, relative to the untreated group ($n = 3$, biological replicates). Data are presented as mean values ± SEM. Two-tailed paired Student's *t*-test. **C** BMMCs from HD (left) and PRCA (right) were cultured in a serum-free erythroid medium, with or without lenalidomide (LENA). Flow cytometry analyses were performed on days 8 and 16. **D** Apoptosis assay on BMMCs cultured for 9 days in erythroid medium, using 4′,6-diamidino-2-phenylindole (DAPI) and Annexin-V. **E** Quantification of cells from panel (**D**) undergoing early and late apoptosis(apop.) ($n = 3$, biological replicates). Data are presented as mean values ± SEM. Two-tailed paired Student's *t*-test. **F** Colony-forming assays of BMMCs from PRCA or HD with indicated treatments. Quantification of BFU-E, CFU-GM, and CFU-GEMM were performed on day 14 ($n = 3$, biological replicates). Data are presented as mean values ± SEM. Two-tailed paired Student's *t*-test. **G** Percentage of BFU-E colonies in each group ($n = 3$, biological replicates). Data are presented as mean values ± SEM. Two-tailed paired Student's *t*-test. Source data are provided as a Source Data file.

percentages of B cell lineage and plasma cells had significantly decreased in the patient's bone marrow, confirming the remission state of multiple myeloma (Supplemental Fig. 4A, B). scRNA-Seq revealed a relative increase in the percentage of $CD8^+$ T cells in the patient, which is consistent with previous reports (Supplemental Fig. 4B, C)[28–30]. We further conducted clustering of T cells, which revealed an increase in the relative percentages of $CD8^+$ memory and cytotoxic cells in the patient, exhibiting elevated cytotoxicity (Supplemental Fig. 4D). Consistent with our analysis in Fig. 1C–E, $CD71^+$ erythroid cells in the patient's bone marrow were significantly reduced, although there were no significant changes in HSPCs (Supplemental Fig. 4E, F). Moreover, the patient's erythroid cells were primarily concentrated in the progenitor stage, characterized by the expression of genes such as *GATA2, CD34*, and *KIT* (Fig. 3C). Conversely, the patient had a lower percentage of erythroblasts, which typically express the genes such as hemoglobin gene *HBB* and *GYPA* (Supplemental Fig. 4G, H). Gene set enrichment analysis (GSEA) revealed that cell cycle and development-related pathways were downregulated in erythroid cells of PRCA, indicating aberrant erythroid development and proliferation. In contrast, the patient's erythroid progenitors exhibited a marked activation of immune-related pathways, including those for MHC-I-mediated antigen presentation (Fig. 3D). This activity extended from proteasome and peptide transport genes to peptide-loading complex (PLC) genes and MHC-I heterodimer molecules (Fig. 3E). Notably, erythroid cells showed the greatest fold increase in MHC-I upregulation compared to other cell types (Supplemental Fig. 5A). These alterations in transcriptional profiles suggested the involvement of an abnormal immune activation mechanism in erythroid progenitors and precursors (Supplemental Fig. 5B, C).

Indeed, unlike the usual decline in MHC-I gene expression seen from progenitors to precursors in HDs, the patient's erythroid precursors sustained a high expression of MHC-I genes. Flow cytometry analyses revealed that the protein level of MHC-I molecules on the surface of $CD235a^+$ erythroblasts in the patient is significantly higher compared to those in HDs (Fig. 3F). In addition, we collected peripheral blood samples from another patient with multiple myeloma who developed PRCA after lenalidomide treatment[31]. Consistent with our

https://doi.org/10.1038/s41467-024-54571-w

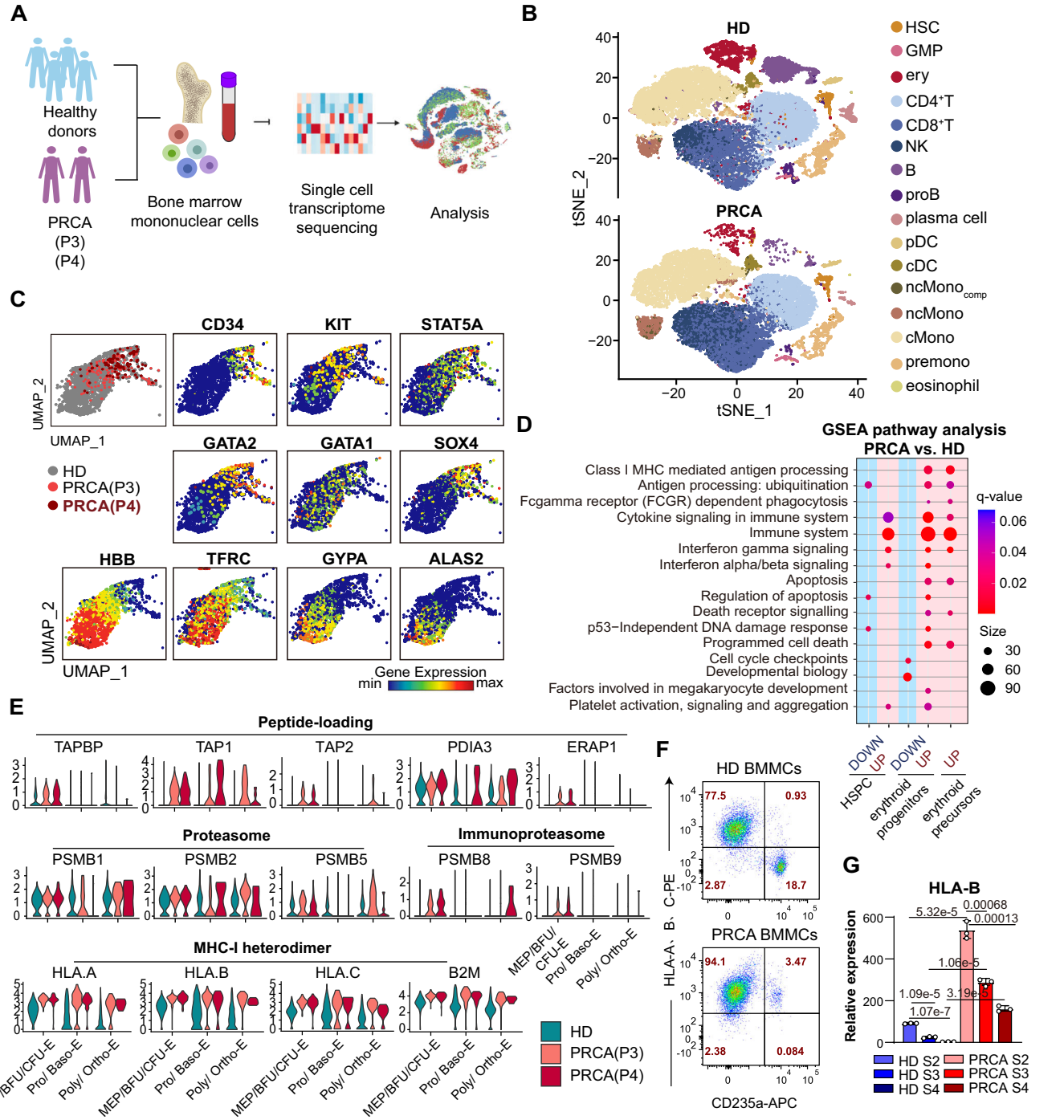

Fig. 3 | MHC-I genes were increased in erythroid cells of PRCA. A Experimental scheme for the analysis of clinical samples. **B** Overview of cell clusters in integrated single-cell transcriptomes derived from BMMCs of healthy donors (HD, upper) and the PRCA patient (lower). Clusters were named based on cluster-specific gene expression patterns. (HSPC hematopoietic stem and progenitor cell, GMP granulocyte–monocyte progenitors, ery erythroid cells, NK natural killer cells, pDC plasmacytoid dendritic cells, cDC conventional (classical) dendritic cells, $ncMono_{comp}$ $C1QA^+/CD16^+$ complement-expressing non-classical monocytes, ncMono $CD14^{dim}CD16^+$ non-classical monocytes, cMono $CD14^{++}CD16^+$ classical monocytes). **C** UMAP analysis of erythroid cells. HD and PRCA samples were combined and colored according to the donor. Expression levels of erythroid markers were used to determine cell stages. **D** GSEA pathway enrichment results for different cell types. The dot color represents the *q*-value; the dot size represents the number of genes related to the indicated pathway. To enable a more accurate comparison of transcriptional differences, we reduced the number of cells in the HD samples to match those in the PRCA samples (as detailed in "Methods"). **E** Expression levels of antigen processing and peptide loading genes, proteasome and immunoproteasome genes, and MHC-I heterodimer genes in erythroid cells based on scRNA-Seq. Erythroid lineage-related cells were divided based on specific markers into progenitor cells (including megakaryocyte–erythroid progenitor cells (MEP), BFU-E and colony-forming unit-erythroid (CFU-E)), early precursor cells (consisting of proerythroblasts and basophilic erythroblasts (Pro/Baso-E)), and late precursor cells (consisting of polychromatic erythroblasts and orthochromatic erythroblasts (Poly/Ortho-E)). **F** Representative flow cytometry results showing MHC-I levels on erythroid cells in the bone marrow from HD (upper) and the PRCA patient (lower). **G** Relative expression levels of HLA-B, detected by quantitative RT-PCR. BMMCs from HD and PRCA patients were cultured in erythroid differentiation medium and sorted into specific stages based on CD71 and CD235a expression by FACS: $CD71^+CD235a^-$ (S2), $CD71^+CD235a^+$ (S3), and $CD71^-CD235a^+$ (S4) ($n = 3$, biological replicates). Data are presented as mean values ± SEM. Two-tailed paired Student's *t*-test. Source data are provided as a Source Data file.

observation in the bone marrow, MHC-I upregulation in erythroid cells was also evident in the peripheral blood samples of both MM patients with induced PRCA after treatment. However, this phenomenon was not present in typical RVd-treated MM patients who did not develop PRCA after RVd treatment (Supplemental Fig. 6).

In vitro cell cultures showed that even the terminally differentiated $CD71^{-}CD235a^{+}$ erythroblasts from the patient persistently manifested a pronounced up-regulation of HLA-B expression (Fig. 3G).

Lenalidomide induces an increase in MHC-I molecules and upregulation of related genes in PRCA erythroblasts

We next tested whether lenalidomide can induce the expression of MHC-I on erythroid cells directly. To test that, BMMCs from the patient or HDs were cultured under conditions that supports erythroid differentiation (Fig. 4A). The addition of lenalidomide resulted in further elevation in the expression of MHC-I molecules on the patient's $CD71^{+}CD235a^{+}$ erythroblasts without any effect on those cells of HD's (Fig. 4B). To elucidate the mechanism underlying defective erythropoiesis in the PRCA patient, we isolated $CD71^{+}$ erythroid progenitors after 6 days of in vitro erythroid differentiation of BMMC with or without lenalidomide for bulk RNA sequencing (Supplemental Fig. 7).

We compared the fold changes of DEGs after lenalidomide addition between cells from HDs and those from the patient (Fig. 4C). Genes that exhibited greater up-regulation after lenalidomide addition in the patient's cells were regarded as "PRCA-specific upregulated genes", while genes that displayed greater downregulation after lenalidomide addition in the patient's cells were regarded as "PRCA-specific downregulated genes." In total, there were 1629 PRCA-specific upregulated genes and 1276 PRCA-specific downregulated genes. In consistency with scRNA-seq results, GSEA analysis showed that upregulated genes of the PRCA patient treated with lenalidomide are involved in antigen presentation, immune pathways as well as cell death, whereas down-regulated genes are related to cell cycle and DNA replication (Fig. 4D). Genes encoding MHC proteins and factors involved in antigen presenting pathways, are upregulated significantly in erythroid cells from the patient with the addition of lenalidomide (Fig. 4E). Lenalidomide might augment IL-2 receptor levels in the patient's erythroid progenitors, thereby bolstering the cellular responses to IL-2 and IFNs, leading to an upregulation of transcription factor genes such as *NLRC5* and *IRF1*[32] These results confirmed the disruptive role of lenalidomide in erythropoiesis, which might be through upregulation of MHC molecules and antigen-presenting pathways.

Proteomic analysis reveals the activation of MHC-I and ubiquitination pathways in PRCA patients

Lenalidomide was identified to promote the ubiquitination and degradation of specific substrates[23,24]. To further examine the role of lenalidomide in PRCA, we performed micro-proteomics analysis on $CD71^{+}$ erythroid progenitor cells sorted by FACS after 6 days of erythroid culture. The inter-sample analysis was conducted based on the results of mass spectrometry (Fig. 4A and Supplemental Data 1). Differential gene clustering analysis of the detected proteins yielded four clusters: Cluster 1 and Cluster 4 contained proteins that were significantly more abundant in PRCA patients and healthy donors, respectively. Cluster 2 and Cluster 3 contained proteins that were significantly more abundant after in vitro lenalidomide treatment in healthy donor and PRCA patient cells, respectively (Fig. 5A).

Further comparison of the differentially enriched proteins in these clusters revealed that the ubiquitin-mediated proteolysis pathway is upregulated in PRCA, while the antigen processing and presentation pathway is distinctly upregulated in PRCA after lenalidomide treatment (Fig. 5B). The upregulated proteins in the ubiquitin-related pathway in PRCA include various E1 activating enzyme, E2 ubiquitin-conjugating enzymes, E3 ubiquitin-protein ligases (including the Cullin ubiquitin ligases), and E4 ubiquitin conjugation factors (Fig. 5C).

The MHC-I pathway enriched in Cluster 3 includes proteins involved in the peptide-loading complex (PLC), MHC-I heterodimer, and proteasome required for peptide degradation, with a notable enrichment of proteins related to the immunoproteasome (i.e., PSMB8, PSMB9, and PSMB10). The levels of these proteins were further upregulated in PRCA cells after the addition of lenalidomide, whereas no significant changes were observed between lenalidomide-treated and untreated BMMCs from healthy donors (Fig. 5D).

Collectively, the proteomic analysis reveals higher levels of ubiquitination-related pathway protein expression in PRCA cells compared to HD. Moreover, the analysis shows upregulation of MHC-I pathway protein expression in PRCA cells, which is further induced by lenalidomide treatment, consistent with our previous findings from single-cell transcriptome analysis.

Blocking of MHC-I-TCR interaction rescues erythropoiesis from the PRCA patient

Interestingly, we also observed enhanced interactions between $CD8^{+}$ T cells and erythroid cells in the PRCA patient. Notably, $CD8^{+}$ T cells from the patient displayed elevated levels of FAS ligand (FASLG)–FAS interactions, which can directly induce apoptosis of erythroid cells (Fig. 6A). Single-cell RNA-seq analysis revealed that, compared to HDs, T cells, particularly $CD8^{+}$ T cells, were hyperactivated in the patient (Fig. 6B, C).

To confirm the role of T cells in PRCA, BMMCs from HDs and the PRCA patient were depleted of T cells before being cultured in the erythroid medium. Our results showed that while T cell depletion did not yield any effect on cell proliferation from HDs, it markedly alleviated defective erythroid proliferation and differentiation in PRCA cells (Fig. 6D, E).

In addition, a marked enhancement of interactions between MHC-I and CD3 was observed (Fig. 6A). MHC-I serves an essential ligand that engages with TCR on the surface of T cells[33,34]. The increased expression of MHC-I on erythroid cells enables us to hypothesize that targeting MHC-I-TCR interaction might rescue defective erythropoiesis in PRCA. To test that, we added antibodies specific for HLA-A, B, and C of MHC-I into the erythroid culture of BMMCs[35]. After a 9-day culture period, it was evident that the addition of HLA antibody considerably promoted the differentiation of the erythroid lineage in PRCA but not in HDs (Fig. 6F, G; Supplemental Fig. 8). We also observed a significant decrease in the percentage of apoptotic erythroid cells from the patient. Therefore, blocking the MHC-I-TCR interaction alleviates erythropoiesis, indicating that the MHC-I-TCR interaction is essential for impaired erythropoiesis in the PRCA patient.

Discussion

PRCA is a hematopoietic disorder characterized by abnormal development of the erythroid lineage. While more than 50 drugs have been reportedly associated with PRCA[8,9], the mechanism underlying drug-induced PRCA remains unclear[13]. Here, we present a case of a patient with multiple myeloma who developed PRCA symptoms after RVd therapy. Functional in vitro experiments revealed that lenalidomide was a key factor contributing to erythropoiesis impairment in this patient. Remarkably, there is an abnormal overexpression of MHC-I on PRCA erythroblasts, and lenalidomide exacerbated the already elevated expression of MHC-I on the surface of erythroblasts, which may further promote their clearance by $CD8^{+}$ T cells. T cells have been the focus of research in autoimmune diseases, while the role of erythroblasts in these diseases is often overlooked[28,36,37]. In this study, we elucidated the mechanism of drug-induced PRCA in a rare case, thus accentuating the role of aberrant erythroblasts expressing immune markers in the pathogenesis of PRCA.

https://doi.org/10.1038/s41467-024-54571-w

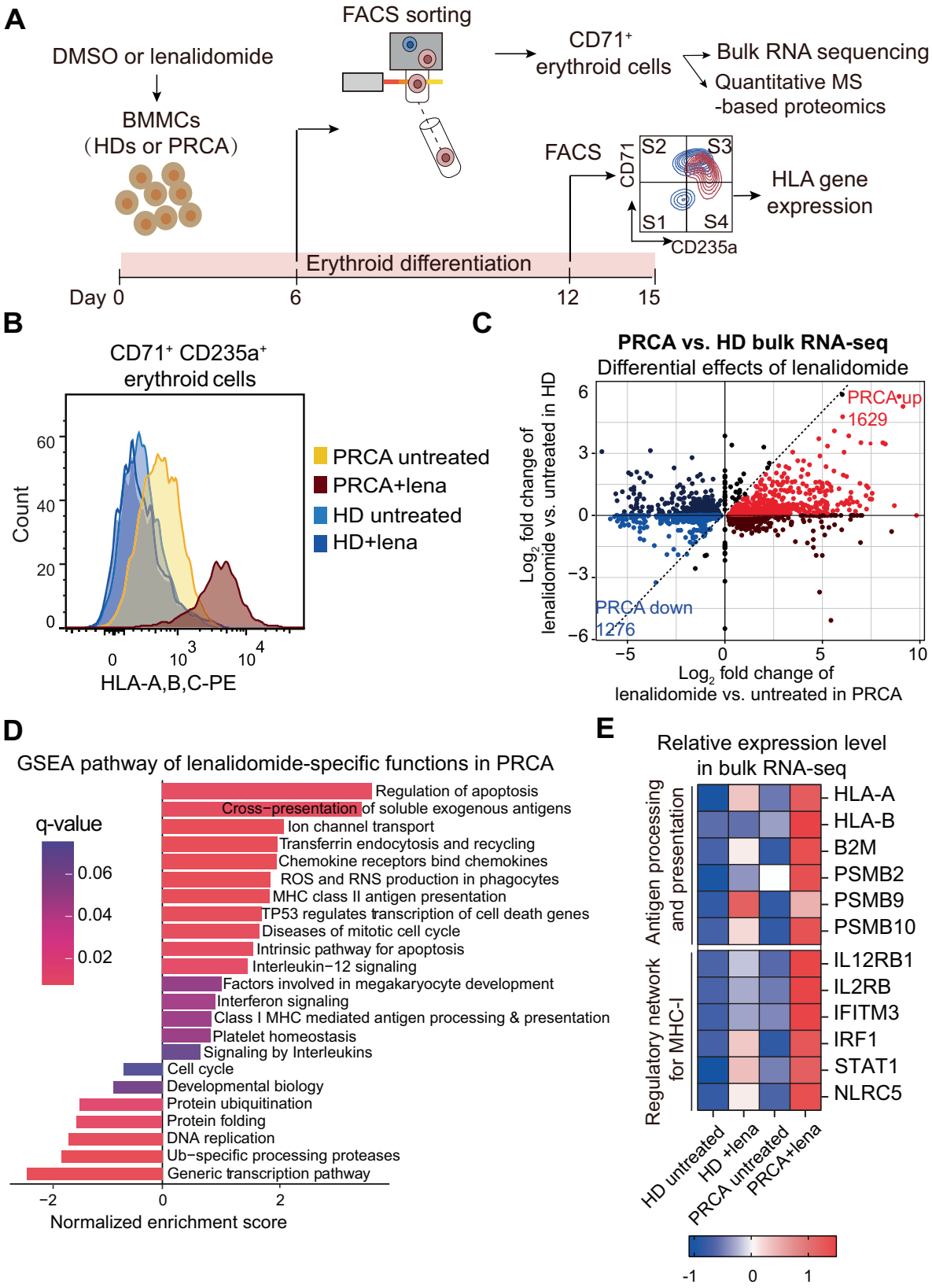

Fig. 4 | Lenalidomide induced elevation of MHC-I expression levels in erythroblasts from PRCA. A Experimental scheme for the analysis of the drug function. **B** Histogram of MHC-I level on CD71$^+$CD235a$^+$ erythroblasts after 12 days of culture in the groups of untreated BMMCs and BMMCs with lenalidomide (all BMMCs from PRCA or HD). **C** Volcano plot of differentially expressed genes (DEGs) after lenalidomide treatment. The *y*-axis shows DEGs in BMMCs from the PRCA patient; the *x*-axis represents DEGs after lenalidomide addition, compared with untreated BMMCs from HD. The slope of the auxiliary line is 1. PRCA-specific unregulated or downregulated genes are shown in red and blue, respectively. **D** Top GSEA pathway enrichment results for PRCA-specific genes. Normalized enrichment scores (NES) are shown, with the color denoting the FDR *q*-value. **E** Relative expression levels of antigen processing and presentation and regulatory network for MHC-I related genes, detected in bulk RNA-seq. Source data are provided as a Source Data file.

https://doi.org/10.1038/s41467-024-54571-w

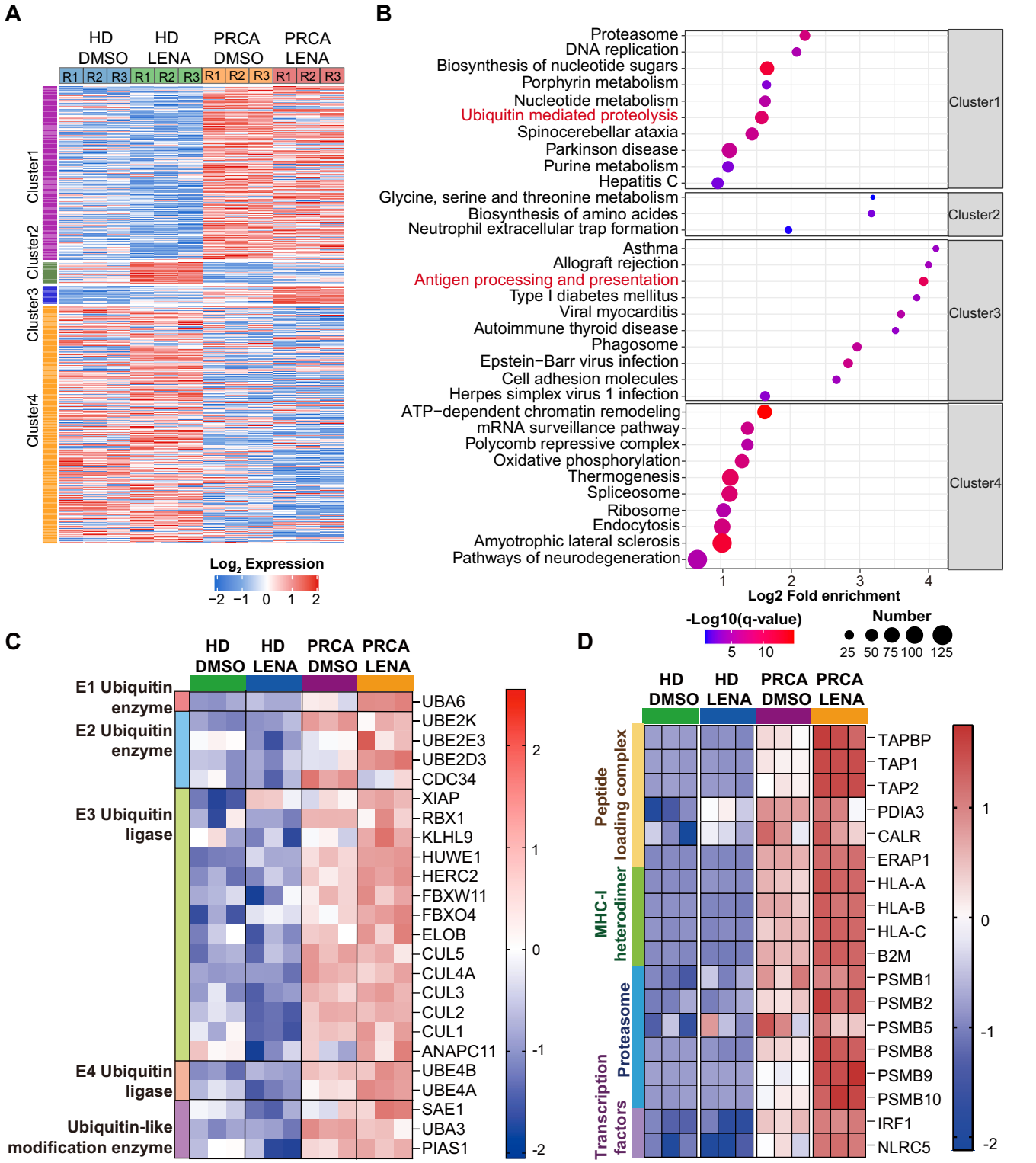

Fig. 5 | Proteomics analysis reveals the activation of MHC-I and ubiquitination pathways in PRCA. A Heatmap of proteins detected by micro-proteomics analysis. Clusters 1–4 were identified by hierarchical clustering. **B** KEGG pathway enrichment results for different clusters. Fisher's exact test was used for data analysis, with adjustments made for multiple comparisons. The dot color represents the −Log10 *q*-value; the dot size represents the number of genes related to the indicated pathway. **C** Relative protein levels of ubiquitin-related genes, detected in micro-proteomics analysis. **D** Relative protein levels of antigen processing and presentation and the regulatory network for MHC-I related genes, detected in micro-proteomics analysis. Source data are provided as a Source Data file.

Consistent with previous studies in aplastic anemia and PRCA[1,2,30,38], we observed a relative enrichment of $CD8^+$ T cells. Since this patient was not diagnosed with thymoma, and flow cytometry did not reveal the clonal expansion of any TCR subtype, we speculate that the patient's abnormal transcriptional status may suggest genomic abnormalities in the $CD8^+$ T cells, potentially contributing to drug-induced proliferation and hyperactivation in the bone marrow. Further genomic analyses and functional assays will be needed

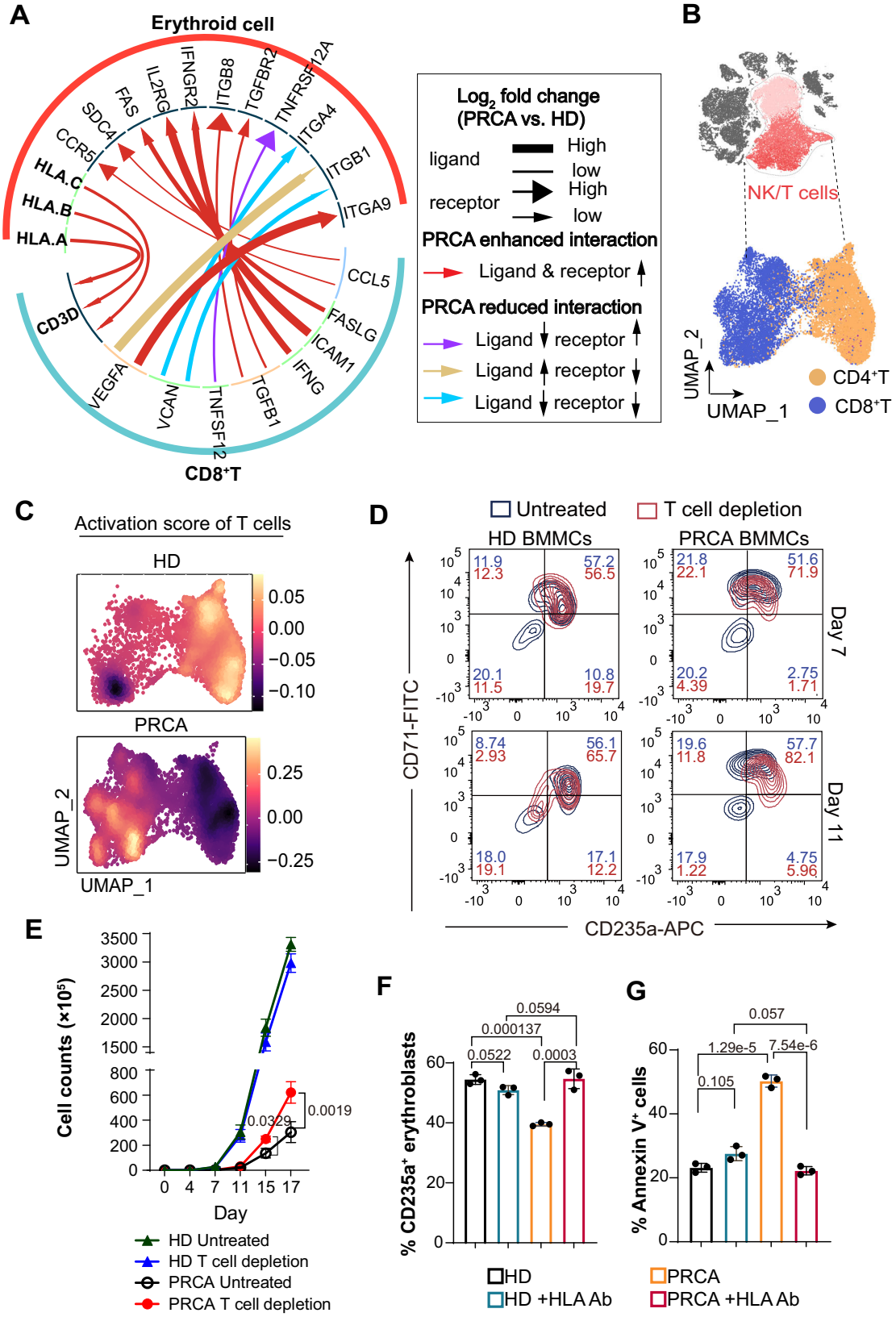

to address this possibility. Cyclosporin A, despite its known T-cell suppressive effects[39–41], was ineffective in treating this PRCA patient's relapse, suggesting the involvement of non-T-cell factors in this pathological process. Elevated IFN-γ levels, detected through transcriptomic and serum analyses, are recognized to hinder erythroid progenitor differentiation[42–44]. Thus, the increased IFN-γ concentration in the patient's serum likely acted as an obstacle to erythropoiesis.

Interestingly, we uncovered an unexpected upregulation of MHC-I-related genes in the patient's erythroid cells, as revealed by both the transcriptome and proteomics analyses. MHC-I molecules are normally absent from the surface of mature erythrocytes. During

Fig. 6 | Blocking MHC-I or T cell depletion rescued erythropoiesis of PRCA. **A** Circle plot showing changes in the interaction intensity of ligand–receptor pairs between $CD8^+$ T cells and erythroid cells in PRCA vs. HD samples. **B** UMAP plot of annotated clusters from T cells ($n = 16{,}000$) in PRCA and HD BMMC samples. **C** Cytotoxicity scores in T cells from the PRCA patient and HD. **D** BMMCs from the PRCA patient (left) and HD (right) were cultured in a serum-free erythroid medium, with or without T-cell depletion. Flow cytometry analyses were performed on days 7 and 11. **E** Cell proliferation curve demonstrating effects of T cells on erythropoiesis. Cell numbers were counted every 4 days, from three independent biological replicates. Data are presented as mean values ± SEM. Two-tailed paired Student's *t*-test. (*$P < 0.05$). **F**, **G** BMMCs from HD and PRCA were cultured in the coculture medium, with or without anti-HLA class I antibody (Ab). $CD235a^+$ erythroid cells (**F**) and cells undergoing apoptosis (**G**) were measured on day 9 ($n = 3$, biological replicates). Data are presented as mean values ± SEM. Two-tailed paired Student's *t*-test. Source data are provided as a Source Data file.

erythroid development, MHC-I-related genes are progressively downregulated[45,46]. Nonetheless, erythrocytes have the capacity to express antigen-presenting molecules under specific pathological conditions[47]. Such a response is noted in erythrocytes when infected with the malaria parasite, which can activate MHC molecule-mediated $CD8^+$ T cell recognition. This activation leads to the externalization of phosphatidylserine and subsequent phagocytosis of the implicated erythrocytes[48]. Additionally, enhanced MHC-I expression on erythrocytes has been observed in patients suffering from systemic lupus erythematosus (SLE), with a correlation to the severity of the disease[49]. These findings imply that erythrocytes may play a supporting role in immune regulation, yet the full extent of their impact on immune cell activity is still to be determined.

In our study, we found elevated expression of HLA genes in both erythroid progenitors and precursors in the PRCA patient's bone marrow. Even the terminal differentiated $CD71^-CD235a^+$ erythroid cells from the patient, a high level of HLA-B was maintained. Moreover, the addition of lenalidomide appeared to promote the sustained high expression levels of MHC-I-related genes in the PRCA patient's cells, a phenomenon not observed in cells from healthy donors. The unique transcriptional status of MHC-I genes, especially *HLA-B*, in the patient's erythroid progenitors, along with the differential response to drugs, likely play a major role in the disrupted erythropoiesis. This is supported by our finding that MHC-I-specific antibodies could substantially restore the defective erythroid differentiation of PRCA cells. Additionally, adverse reactions to drugs in populations with specific MHC-I subtypes have been reported in various diseases[50–52]. Whether the adverse reactions of lenalidomide are associated with this HLA-B subtype still requires exploration with more clinical case data.

Regarding the erythroid-selective cytotoxic effects of hyperactive $CD8^+$ T cells in PRCA, our scRNA-seq analysis revealed a plethora of T cell inhibitory genes, such as *SERPINB9*, *LILRB4*, and *LGALS1*[53–56], which are highly expressed in dendritic cells and monocytes, but not in erythroid cells of PRCA. These observations may explain the targeted cytotoxicity of hyperactive $CD8^+$ T cells towards erythroid cells in PRCA.

In conclusion, we have comprehensively interrogated the mechanism of lenalidomide-induced PRCA, focusing on the perspective of erythroid cells. While we have identified extrinsic factors, including $CD8^+$ T cells and serum factors like IFN-γ play disruptive roles in erythropoiesis, intrinsic defects of erythroid progenitors also contribute to PRCA development. Moreover, we unveiled a mechanism involving elevated HLA expression in PRCA erythroblasts. Our findings suggest that the MHC-I molecule may serve as a crucial clinical marker for other PRCA cases. Detecting abnormal MHC-I levels in erythroblasts or other cells should prompt caution when considering the use of immunomodulatory drugs like lenalidomide to prevent potential adverse reactions.

Methods

Human sample collection and ethics statement

BM and peripheral blood samples from healthy donors (3 males and 1 female), multiple myeloma patients (3 males and 1 female), and PRCA patients (2 males) were collected at Peking University People's Hospital and Peking Union Medical College Hospital. Gender was not considered in the study design due to the limitation of the sample size. All samples were collected after informed consent had been obtained, in accordance with the Declaration of Helsinki, under a protocol approved by the Research Ethics Board at Peking University Health Science Center and People's Hospital. Bone marrow cells and peripheral blood cells were diluted 1:1 in ice-cold phosphate-buffered saline (PBS). Mononuclear cell separation was performed using density centrifugation media (Ficoll–Paque; GE Healthcare Life Sciences, Cat. # 07851) at a 1:1 ratio with diluted blood or marrow cells. After centrifugation (1200×*g*, 10 min), mononuclear cells were carefully aspirated to lyse red blood cells.

Human cord blood cells were obtained from the Cord Blood Bank of Beijing. After monocytes had been extracted from cord blood, $CD34^+$ cells were isolated via magnetic-activated cell sorting technology using a MicroBead kit (Miltenyi, Cat. # 130-100-453).

Ex vivo BMMC erythroid culture

BMMCs were cultured in Serum-Free Expansion Medium II (SFEM II) based erythroid differentiation medium. The medium also contained 3 IU/ml erythropoietin (Amgen, Cat. #55513-144-10), 10 ng/ml hIL-3 (StemCell Technologies, Cat. #78042), and 50 ng/ml human stem cell factor (StemCell Technologies, Cat. #78062). When testing the effects of drugs on cells,10 nM bortezomib, 250 nM lenalidomide, or 250 nM dexamethasone was added to the medium. Cell differentiation was determined by flow cytometry analyses of erythroid markers, including CD71, CD235a, and Hoechst 33342.

Colony-forming assays

For colony-forming assays involving BMMCs, 20,000 cells were plated in each well of a 6-well plate using MethoCult H4435 Optimum (StemCell Technologies). For colony-forming assays involving human $CD34^+$ cells, 200 cells in MethoCult H4435 Optimum (StemCell Technologies) were plated in each well of a 6-well plate. In experiments to determine the effects of serum and drugs, drugs and 10% serum were added to the medium on day 0. Cells were cultured for 14 days; subsequently, BFU-E, CFU-GM, and CFU-GEMM colonies were counted and scored.

T cell isolation

T cells were isolated from BMMCs of the patient or healthy donors. The mouse anti-human CD3-BV650 (BD, clone SK7) and mouse anti-human CD8a-FITC (BD, clone HIT8a) were used to identified T cells. $CD3^+$ cells were isolated using a FACS AriaIII flow cytometer (BD Biosciences).

Inhibition of MHC-I interaction in total BMMC cultures

BMMCs were cultured in SFEM II medium formulated for erythroblast and T cell coculture. This medium was supplemented with 3 IU/ml of erythropoietin (Amgen, Cat. #55513-144-10), 10 ng/ml human IL-3 (StemCell Technologies, Cat. #78042), 50 ng/ml human stem cell factor (StemCell Technologies, Cat. #78062), 10 ng/ml recombinant IL-2 (Peprotech, 200-02), and 2 μg/ml anti-CD28 (BD Biosciences, Cat. #555725). An anti-human HLA-A, B, C antibody (BioLegend, Cat. #311402) at a concentration of 1 μg/ml was introduced to inhibit the interaction between the HLA class complex and $CD8^+$ T cells. Post 16 h of incubation, cells were intracellularly labeled with fluorophore-conjugated antibodies against CD4, CD8, Granzyme B (GzmB), and IFNγ and analyzed with a BD LSR Fortessa flow cytometer. The culture medium was refreshed every 3 days. On day 7, cell apoptosis rates were

quantified by flow cytometry after staining with fluorophore-conjugated anti-CD4, anti-CD8, and anti-CD235a antibodies.

scRNA-Seq experiment

Single-cell capture was achieved by the BD Rhapsody system. Whole transcriptome libraries were prepared according to the BD Rhapsody single-cell whole-transcriptome amplification workflow and sequenced using HiSeq Xten (Illumina, San Diego, California, USA) on a 150 bp paired-end run. Raw data were processed using fastQ to filter adaptor sequences and remove low-quality reads. The cell barcode whitelist was identified by UMI tools. The UMI-based clean data were mapped to the human reference genome (Ensemble V.91) using the STAR algorithm. UMI count matrices were generated for each sample, and imported into the Seurat R toolkit (V. 4.1.3). Cluster analysis was performed by Seurat.

Cell–cell communication analysis using iTALK

The R package iTALK[57] was used to identify and visualize possible cell-cell interactions and to quantify differences between the PRCA patient and healthy donors. Three hundred and twenty cytokine/chemokine ligand–receptor pairs from the database were analyzed. The Wilcoxon rank-sum test was employed to identify differentially expressed genes (DEGs) between the PRCA patient and healthy donors for each cell type. Subsequently, the ligand–receptor database was paired and matched to construct a putative cell–cell communication network. An interaction score was defined as the product of the $\log_2$ (fold change) of the ligand and receptor.

Unsupervised clustering, marker identification, and cell type annotation

The Seurat package (with default settings) was used for the normalization and scaling of the expression matrix. Mitochondrial contamination was regressed by adjusting the "vars.to.regress" parameter. To reduce expression matrix dimensionality, principal component analysis was performed based on 2000 highly variable genes. Unsupervised cell clusters were acquired using a graph-based clustering approach (i.e., the top 20 principal components were selected with a resolution of 0.75), then visualized by uniform manifold approximation and projection (UMAP) or t-Distributed Stochastic Neighbor Embedding (t-SNE) dimensionality reduction. Clusters were annotated to known biological cell types according to the expression patterns of canonical markers. Marker genes in each cluster were identified using the FindAllMarkers function with the following criteria: log (fold change) > 0.25, min. pct > 0.25, and adjusted *P*-value < 0.05. Pathway analysis was used to identify significant pathways of DEGs according to the Kyoto Encyclopedia of Genes and Genomes (KEGG) and GSEA database.

To enable a more accurate comparison of transcriptional differences between HD and PRCA samples, we used Seurat's 'downsample' function to randomly reduce the HD sample to 300 HSC cells, 200 erythroid progenitor cells, and 60 erythroid precursor cells, matching the cell numbers in the PRCA samples (Supplemental Fig. 5B, C). The differential gene analysis (Supplemental Fig. 5B, C) informed the GSEA pathway enrichment analysis in Fig. 3D.

Bulk RNA-seq

After treatment with indicated drugs in an erythroid differentiation medium for 6 days. Cells were spun down and resuspended in the staining buffer (2% FBS in PBS); then the 5 µl anti-CD235a (APC, clone HIR2, eBioscience, Cat.# 17-9987-42), 5 µl anti-CD71 (FITC, clone OKT9, eBioscience, Cat.#11-0719-42) were added as per 1,000,000 cells. FACS sorting was performed on BD FACSAria III. The $CD71^+$ erythroid progenitor cells were sorted by fluorescence-activated cell sorting (FACS). The cell populations of $CD71^+$ differentiation stages were isolated. RNA was extracted with TRIzol and cleaned with an RNeasy MinElute Cleanup Kit.

RNA was extracted using the RNA isolation Total RNA Extraction Reagent (Vazyme, Cat.# R401-01). Sequencing libraries were prepared by Novogene, and 150 bp paired-end sequencing of each condition with two biological replicates was obtained in a HiSeq X-Ten (PE150, Illumina) by Novogene (Beijing). FASTQ files were generated by Novogene. Hisat2 (version 2.1.0) was used to align the paired-end raw data human reference genome, HTSeq was used to calculate the reads counts, and DESeq2 was used to identify the differential expression genes.

Proteomics analysis

As described above, $CD71^+$ erythroid cells were sorted by FACS after six days of in vitro culture. The sample was sonicated three times on ice using a high-intensity ultrasonic processor (Scientz) in lysis buffer (8 M urea, 1% protease inhibitor cocktail). The remaining debris was removed by centrifugation. The protein concentration was determined using a bicinchoninic acid (BCA) protein assay kit. For digestion, the protein solution was reduced with 5 mM dithiothreitol for 30 min at 56 °C and alkylated with 11 mM iodoacetamide for 15 min at room temperature in darkness. The protein sample was then diluted by adding 200 mM TEAB to reduce the urea concentration to less than 2 M. Trypsin was added at a 1:50 trypsin-to-protein mass ratio for the first digestion overnight, followed by a second 4 h-digestion. Finally, the peptides were desalted by the Strata X SPE column. LC–MS/MS Analysis was conducted at Jingjie PTM Biolab (Hangzhou).

Statistics

Statistical analyses were performed using the Prime 10 software (Graphpad, La Jolla, CA). We considered *P* values of less than 0.05 to be statistically significant. Data are expressed as the mean ± standard deviation. A two-tailed unpaired/paired Student's *t*-test was performed for the comparison between two groups (ns, $P > 0.05$; *, $P \le 0.05$; **, $P \le 0.01$; ***, $P \le 0.001$).

Reporting summary

Further information on research design is available in the Nature Portfolio Reporting Summary linked to this article.

Data availability

The data in this paper have been deposited in the Genome Sequence Archive of the National Genomics Data Center. The assigned accession number of the submission is HRA006868. The raw data are available under controlled access due to data privacy laws related to patient consent for data sharing. The data should be used for research purposes only. According to the guidelines of GSA-human, all non-profit researchers are allowed access to the data, and the Principal Investigator of any research group can apply for the data following the guidelines at the GSA database portal (https://ngdc.cncb.ac.cn/gsa-human/). The response time for access requests is approximately 8 working days. Once access has been granted, the data will be available for download within one month. The user can also contact the corresponding author directly for inquiries. The mass spectrometry proteomics data have been deposited to the ProteomeXchange Consortium (https://proteomecentral.proteomexchange.org) via the iProX partner repository with the dataset identifier PXD055495. Source data are provided in this paper.

Code availability

The R scripts used for single-cell RNA sequencing data analysis are available at https://github.com/Swiftion/single-cell-rna-seq-for-lenalidomide-induced-PRCA.

References

1. Gurnari, C. & Maciejewski, J. P. How I manage acquired pure red cell aplasia in adults. *Blood* **137**, 2001–2009 (2021).

2. Sawada, K., Fujishima, N. & Hirokawa, M. Acquired pure red cell aplasia: updated review of treatment. *Br. J. Haematol.* **142**, 505–514 (2008).
3. Brown, K. E. et al. Resistance to parvovirus B19 infection due to lack of virus receptor (erythrocyte P antigen). *N. Engl. J. Med.* **330**, 1192–1196 (1994).
4. Frickhofen, N. et al. Parvovirus B19 as a cause of acquired chronic pure red cell aplasia. *Br. J. Haematol.* **87**, 818–824 (1994).
5. Bernard, C. et al. Thymoma associated with autoimmune diseases: 85 cases and literature review. *Autoimmun. Rev.* **15**, 82–92 (2016).
6. Gurnari, C. et al. Novel invariant features of Good syndrome. *Leukemia* **35**, 1792–1796 (2021).
7. Sanikommu, S. R. et al. Clinical features and treatment outcomes in large granular lymphocytic leukemia (LGLL). *Leuk. Lymphoma* **59**, 416–422 (2017).
8. Means, R. T. Pure red cell aplasia. *Blood* **128**, 2504–2509 (2016).
9. Thompson, D. F. & Gales, M. A. Drug-induced pure red cell aplasia. *Pharmacotherapy* **16**, 1002–1008 (1996).
10. Mariette, X. et al. Rifampicin-induced pure red cell aplasia. *Am. J. Med.* **87**, 459–460 (1989).
11. Dessypris, E. N., Redline, S., Harris, J. W. & Krantz, S. B. Diphenylhydantoin-induced pure red cell aplasia. *Blood* **65**, 789–794 (1985).
12. Durie, B. G. M. et al. Bortezomib with lenalidomide and dexamethasone versus lenalidomide and dexamethasone alone in patients with newly diagnosed myeloma without intent for immediate autologous stem-cell transplant (SWOG S0777): a randomised, open-label, phase 3 trial. *Lancet* **389**, 519–527 (2017).
13. O'Donnell, E. K. et al. A phase 2 study of modified lenalidomide, bortezomib and dexamethasone in transplant-ineligible multiple myeloma. *Br. J. Haematol.* **182**, 222–230 (2018).
14. Richardson, P. G. et al. Lenalidomide, bortezomib, and dexamethasone combination therapy in patients with newly diagnosed multiple myeloma. *Blood* **116**, 679–686 (2010).
15. Kumar, S. et al. Randomized, multicenter, phase 2 study (EVOLUTION) of combinations of bortezomib, dexamethasone, cyclophosphamide, and lenalidomide in previously untreated multiple myeloma. *Blood* **119**, 4375–4382 (2012).
16. Gerecke, C. et al. The Diagnosis and treatment of multiple myeloma. *Deutsches Ärzteblatt international* (2016).
17. Chen, Y., Tao, S., Hu, M. & Fu, C. Efficacy and side effects of low-dose lenalidomide combined with PCD and VAD regimens in the treatment of elderly multiple myeloma. *Chin. J. Gerontol.* **42**, 4962–4965 (2022).
18. Voorhees, P. M. et al. Daratumumab, lenalidomide, bortezomib, and dexamethasone for transplant-eligible newly diagnosed multiple myeloma: the GRIFFIN trial. *Blood* **136**, 936–945 (2020).
19. Richardson, P. G. et al. Immunomodulatory drug CC-5013 overcomes drug resistance and is well tolerated in patients with relapsed multiple myeloma. *Blood* **100**, 3063–3067 (2002).
20. Haslett, P. A. J., Corral, L. G., Albert, M. & Kaplan, G. Thalidomide costimulates primary human T lymphocytes, preferentially inducing proliferation, cytokine production, and cytotoxic responses in the $CD8^+$ subset. *J. Exp. Med.* **187**, 1885–1892 (1998).
21. Davies, F. E. et al. Thalidomide and immunomodulatory derivatives augment natural killer cell cytotoxicity in multiple myeloma. *Blood* **98**, 210–216 (2001).
22. LeBlanc, R. et al. Immunomodulatory drug costimulates T cells via the B7-CD28 pathway. *Blood* **103**, 1787–1790 (2004).
23. Krönke, J. et al. Lenalidomide causes selective degradation of IKZF1 and IKZF3 in multiple myeloma cells. *Science* **343**, 301–305 (2014).
24. Krönke, J. et al. Lenalidomide induces ubiquitination and degradation of CK1α in del(5q) MDS. *Nature* **523**, 183–188 (2015).
25. Dolai, T. K., Dutta, S., Mandal, P. K. & Saha, S. Bhattacharyya M. Lenalidomide-Induced Pure Red Cell Aplasia. *Turk. J. Hematol.* **31**, 99–100 (2014).
26. Ito, T. et al. Secondary pure red cell aplasia in multiple myeloma treated with lenalidomide. *Leuk. Res. Rep.* **10**, 4–6 (2018).
27. Flygare, J., Estrada, V. R., Shin, C., Gupta, S. & Lodish, H. F. HIF1α synergizes with glucocorticoids to promote BFU-E progenitor self-renewal. *Blood* **117**, 3435–3444 (2011).
28. Kawakami, F. et al. T cell clonal expansion and STAT3 mutations: a characteristic feature of acquired chronic T cell-mediated pure red cell aplasia. *Int. J. Hematol.* **115**, 816–825 (2022).
29. Fujishima, N. et al. Oligoclonal T cell expansion in blood but not in the thymus from a patient with thymoma-associated pure red cell aplasia. *Haematologica* **91**, Ecr47 (2006).
30. Masuda, M. et al. Clonal T cells of pure red-cell aplasia. *Am. J. Hematol.* **79**, 332–333 (2005).
31. Jin, X. et al. Pure red cell aplasia and minimal residual disease conversion associated with immune reconstitution in a patient with high risk multiple myeloma. *Chronic Dis. Transl. Med.* **9**, 341–344 (2023).
32. Jongsma, M. L. M., Guarda, G. & Spaapen, R. M. The regulatory network behind MHC class I expression. *Mol. Immunol.* **113**, 16–21 (2019).
33. Kotsias, F., Cebrian, I., Alloatti, A. Antigen processing and presentation. In: *Immunobiology of Dendritic Cells Part A*) (2019).
34. Neefjes, J., Jongsma, M. L. M., Paul, P. & Bakke, O. Towards a systems understanding of MHC class I and MHC class II antigen presentation. *Nat. Rev. Immunol.* **11**, 823–836 (2011).
35. Moon, J.-S. et al. Cytotoxic $CD8^+$ T cells target citrullinated antigens in rheumatoid arthritis. *Nat. Commun.* **14**, 319 (2023).
36. Michishita, Y. et al. CDR3-independent expansion of Vδ1 T lymphocytes in acquired chronic pure red cell aplasia. *Immunol. Lett.* **150**, 23–29 (2013).
37. Park, S. et al. Distinct mutational pattern of T-cell large granular lymphocyte leukemia combined with pure red cell aplasia: low mutational burden of STAT3. *Sci. Rep.* **13**, 7280 (2023).
38. Young, N. S., Epstein, F. H. & Maciejewski, J. The pathophysiology of acquired aplastic anemia. *N. Engl. J. Med.* **336**, 1365–1372 (1997).
39. Liu, J. et al. Calcineurin is a common target of cyclophilin-cyclosporin A and FKBP-FK506 complexes. *Cell* **66**, 807–815 (1991).
40. Frishberg, Y., Meyers, C. M. & Kelly, C. J. Cyclosporine A regulates T cell-epithelial cell adhesion by altering LFA-1 and ICAM-1 expression. *Kidney Int.* **50**, 45–53 (1996).
41. Shi, Y., Sahai, B. M. & Green, D. R. Cyclosporin A inhibits activation-induced cell death in T-cell hybridomas and thymocytes. *Nature* **339**, 625–626 (1989).
42. De Bruin, A. M., Demirel, Ö., Hooibrink, B., Brandts, C. H. & Nolte, M. A. Interferon-γ impairs proliferation of hematopoietic stem cells in mice. *Blood* **121**, 3578–3585 (2013).
43. Yang, L. et al. IFN-γ negatively modulates self-renewal of repopulating human hemopoietic stem cells. *J. Immunol.* **174**, 752–757 (2005).
44. Wang, C. Q., Udupa, K. B. & Lipschitz, D. A. Interferon-γ exerts its negative regulatory effect primarily on the earliest stages of murine erythroid progenitor cell development. *J. Cell. Physiol.* **162**, 134–138 (1995).
45. Bagger, F. O., Kinalis, S. & Rapin, N. BloodSpot: a database of healthy and malignant haematopoiesis updated with purified and single cell mRNA sequencing profiles. *Nucleic Acids Res.* **47**, D881–D885 (2019).
46. Ludwig, L. S. et al. Transcriptional states and chromatin accessibility underlying human erythropoiesis. *Cell Rep.* **27**, 3228–3240.e3227 (2019).

47. Vinetz, J. M. et al. Adoptive transfer of CD8 + T cells from immune animals does not transfer immunity to blood stage *Plasmodium yoelii* malaria. *J. Immunol.* **144**, 1069–1074 (1990).
48. Imai, T. et al. Cytotoxic activities of CD8+ T cells collaborate with macrophages to protect against blood-stage murine malaria. *Elife* **4**, e04232 (2015).
49. Giles, C. M., Walport, M. J., David, J. & Darke, C. Expression of MHC class I determinants on erythrocytes of SLE patients. *Clin. Exp. Immunol.* **69**, 368–374 (1987).
50. Illing, P. T. et al. Immune self-reactivity triggered by drug-modified HLA-peptide repertoire. *Nature* **486**, 554–558 (2012).
51. Norcross, M. A. et al. Abacavir induces loading of novel self-peptides into HLA-B*57. *Aids* **26**, F21–F29 (2012).
52. Ostrov, D. A. et al. Drug hypersensitivity caused by alteration of the MHC-presented self-peptide repertoire. *Proc. Natl Acad. Sci. USA* **109**, 9959–9964 (2012).
53. Huang, Y., Wang, H.-C., Zhao, J., Wu, M.-H. & Shih, T.-C. Immunosuppressive roles of galectin-1 in the tumor microenvironment. *Biomolecules* **11**, 1398 (2021).
54. Medema, J. P. et al. Expression of the serpin serine protease inhibitor 6 protects dendritic cells from cytotoxic T lymphocyte–induced apoptosis: differential modulation by T helper type 1 and type 2 cells. *J. Exp. Med.* **194**, 657–668 (2001).
55. Yang, T., Qian, Y., Liang, X., Wu, J., Zou, M., & Deng, M. LILRB4, an immune checkpoint on myeloid cells. *Blood Sci.* **4**, 49–56 (2022).
56. Jiang, L. et al. Direct tumor killing and immunotherapy through anti-SerpinB9 therapy. *Cell* **183**, 1219–1233.e1218 (2020).
57. Wang, Y. et al. iTALK: an R Package to Characterize and Illustrate Intercellular Communication. *bioRxiv* https://doi.org/10.1101/507871 (2019).

Acknowledgements

We thank the Flow Cytometry Core and the Imaging Core of the National Center for Protein Sciences at Peking University (PKU). We thank the High-Performance Computing Platform of the Center for Life Sciences (PKU) for supporting data analysis. We are grateful to Dr. Hongxia Lyu, Huan Yang, and Xuefang Zhang (PKU) for their technical support. We thank all the other members of the laboratory for their critical reading of this manuscript. This project was supported by grants from the National Key R&D Program of China (2022YFA1103300) to X.H.J. and H.Y.L.; the National Natural Science Foundation of China (82370124) and the Peking-Tsinghua Center for Life Sciences and School of Life Sciences, Peking University, to H.Y.L.; the Zhejiang Provincial Natural Science Foundation of China (LR20C070001), "Leading Goose" R&D Program (2024C03089), and the Science and Technology Department of Zhejiang Province (Key Project, 2021C03011)" to X.G.

Author contributions

Q.H., Y.L., J.L., X.G., and H.Y.L. conceptualized this project and designed the experiments. Q.H., Q.Y.Y., and S.Z. performed the experiments. Q.H. conducted bioinformatic analyses. Q. H., Y.L., Z.J.L., X.H.J., F.L., X.J.H., J.L., X.G., and H.Y.L. wrote the paper. All authors discussed the results and commented on the paper.

Competing interests

The authors declare no competing interests.

Additional information

Supplementary information The online version contains supplementary material available at https://doi.org/10.1038/s41467-024-54571-w.

Correspondence and requests for materials should be addressed to Junling Zhuang, Jin Lu, Xiaofei Gao or Hsiang-Ying Lee.

Peer review information *Nature Communications* thanks Lionel Blanc, Shinichi Hashimoto, and Hirokazu Miki for their contribution to the peer review of this work. A peer review file is available.